Research article

Diminished activity-dependent neuroprotective protein (ADNP) contributes to complement gene elevation in Alzheimer's disease

Journal of Alzheimer's Disease
1–14

DOI: 10.1177/13872877261427770
journals.sagepub.com/home/alz

Yong Ren[1,2,*], Komal Saleem[2,*], Prachetas Jai Patel[2,*], Young-Ho Lee[2], Jian Feng[2] and Zhen Yan[1,2]

Abstract

Background: Gene dysregulation is one of the key mechanisms that link pathological abnormalities to cognitive impairment in Alzheimer's disease (AD), the most prevalent neurodegenerative disorder. Our transcriptomic analysis of large-scale postmortem AD human prefrontal cortex (PFC) data revealed that complement genes, a key player in modulating tissue homeostasis and immune surveillance, were prominently upregulated.

Objective: The goal of this study is to reveal key transcriptional regulators that contribute to the elevation of complement genes in AD.

Methods: Transcriptomic and epigenomic analyses, molecular, biochemical and immunocytochemical assays, and in vivo gene manipulation, were used.

Results: Our epigenomic analysis identified ADNP (activity-dependent neuroprotective protein), a chromatin regulator strongly linked to intellectual disability, as one of the top-ranking transcription factors regulating complement genes. ADNP and its partner HP1γ (Heterochromatin protein 1) were found to be significantly diminished in postmortem AD human PFC. Reduced Adnp expression was also found in PFC of a familial AD mouse model, 5xFAD. Knockdown of Adnp in mice led to the significantly increased levels of complement genes, reminiscent to complement gene elevation in postmortem AD humans and 5xFAD mice. Furthermore, human induced pluripotent stem cell-derived neuronal cultures from AD patients exhibited astrocyte activation, ADNP/HP1γ reduction, and complement gene increase. Manipulation of ADNP levels led to bidirectional changes in complement gene expression.

Conclusions: These data suggest that the diminished ADNP in AD could lead to chromatin dysregulation because of disrupted transcriptional repression, which contributes to the elevation of complement genes. It provides a novel upstream epigenetic modifier for gene dysregulation in AD.

Keywords

activity-dependent neuroprotective protein, ADNP, Alzheimer's disease, complement genes, epigenetics, 5xFAD, induced pluripotent stem cells

Received: 11 November 2025; accepted: 22 January 2026

Introduction

Alzheimer's disease (AD), a prevalent neurodegenerative disorder, is associated with several neuropathological features and converging pathways.[1,2] Multi-omics studies of AD patient postmortem tissues have revealed AD-related molecular networks, including amyloid cascade, inflammation, complement, ion homeostasis and membrane transport.[3] While the transcriptional activation of inflammation-related genes is one prominent feature of

[1]VA Western New York Healthcare System, Medical Research, Buffalo, NY, USA
[2]Department of Physiology and Biophysics, School of Medicine and Biomedical Sciences, State University of New York (SUNY) at Buffalo, Buffalo, NY, USA

[*]These authors contribute equally to this work.

Corresponding author:
Zhen Yan, VA Western New York Healthcare System, 3495 Bailey Avenue, Research Building 20, Buffalo, NY 14215, USA.
Email: zhenyan@buffalo.edu

AD,[4–6] the upstream regulators for the elevation of these genes are largely unknown.

By transcriptomic analysis of large-scale postmortem AD data,[4] we found that the upregulated genes were highly enriched in the complement pathway. The complement system is important in modulating tissue homeostasis and immune surveillance. Disruption of the delicate coordination required for complement activation could lead to pro-inflammation and synaptic loss in AD and other neurological disorders.[7–10] The classical complement pathway begins with activation of the C1 complex consisting of the sensing molecule C1q, which can directly bind to the surfaces of pathogens to initiate first-line defense. C1q is also produced locally in the CNS. C1q activation leads to C3 cleavage and C3b tagging of synapses, which can be recognized by microglia CR3 receptors, leading to synapse elimination.[11] While complement pathway overactivation has emerged as a potentially important contributor to neurodegenerative processes,[7,9,10,12] it remains unclear on how complement genes are elevated in AD.

Our epigenomic analysis suggests that activity-dependent neuroprotective protein (ADNP) is a top-ranking transcription factor regulating the expression of complement genes. ADNP is one of the most significant risk factors for intellectual disability (ID) and autism.[13–16] Emerging evidence shows that ADNP functions as an important chromatin regulator.[17,18] ADNP interacts with the heterochromatin protein 1 (HP1) and chromodomain helicase DNA-binding protein 4 (CHD4) to form a stable complex to mediate gene silencing.[17] By using an AD mouse model and human induced pluripotent stem cell (iPSC)-derived cortical neuronal cultures from AD patients, we have revealed that ADNP expression is decreased in AD, which leads to the elevation of complement genes.

Methods

Postmortem human brain tissues and animals

Postmortem human tissues were provided by NIH NeuroBioBank (Supplemental Table 1). Frontal cortex (Brodmann's Area 10) from AD patients and control subjects was used for RNA and protein extraction.

All animal experiments were performed with the approval of State University of New York at Buffalo Animal Care Committee. The transgenic 5×FAD mice[19] with genetic background of (C57BL/6J x SJL/J) F1 were from Jax Lab. They carry 5 familial AD mutations on human amyloid precursor protein (K670N/M671L + I716V + V717I) and human presenilin 1 (M146L + L286 V). Non-carrier x hemizygote was used for breeding. Genotyping was performed by PCR of tail DNA. PFC, including prelimbic cortex (PL), infralimbic cortex (IL) and anterior cingulate cortex (ACC), of WT versus 5xFAD (8 months old) mice were dissected out for experiments.

To generate Adnp-deficient mice, GFP-tagged Adnp shRNA AAV was injected (0.5 µl per hemisphere) to medial PFC of WT mice (6-month-old) bilaterally using a stereotaxic apparatus (David Kopf Instruments), as we previously described.[20] The coordinates of injection were 2.0-mm anterior to bregma; 0.25-mm lateral; and 2.25-mm dorsal to ventral. A Hamilton syringe was used for the injection (speed: 0.1 µl/min), and the needle was kept in place for an additional 5 min. About 2 weeks after surgery, PFC (PL, IL, ACC) of GFP- versus Adnp shRNA AAV-injected mice were dissected out for experiments.

RNA-Sequencing and bioinformatics analysis

Total RNA was isolated from mouse brains, RNA-seq libraries were prepared with Illumina's TruSeq stranded total RNA plus Ribo-Zero kits and sequenced on a HiSeq 2500 platform. Reads were aligned to the mm10 mouse genome with RNA STAR, and gene expression was quantified using featureCounts, filtering out non-canonical, ribosomal, and mitochondrial genes.

We analyzed a human dorsolateral PFC microarray dataset (GSE44770) comprising 129 AD and 101 control samples via Phantasus, in addition to RNAseq data between WT versus ADNP-deficient mice (GSE188865) and WT versus 5xFAD mice. Differentially expressed genes (DEGs) were identified with DESeq2. DEG lists were interrogated for functional enrichment using EnrichR.[21] A PPI network for top-enriched categories was built in STRING, and hub genes were identified in Cytoscape using CytoHubba. Circos plot was used to visualize DEG magnitude and chromosome location. A scatter plot was applied to the most outer layer representing Log_2(Fold Change). Dots (data points) with significant p-values were highlighted in red (decrease) or blue (increase) for each DEG on each chromosome; the further out the dot is, the more changed in magnitude the differential gene is in either direction. Phantasus-generated heatmap was used to visualize key genes. Interactive Genome Viewer (IGV)[22] was used to display ADNP ChIP-seq landscape from ChIP-Atlas. Overlapping gene sets were analyzed with InteractiveVenn.

Generation of ADNP shRNA and full-length ADNP lentiviruses

The human ADNP shRNA sequence (5′-TAAGCTGGTGA CTCATGAATA-3′) was selected from TRC (RNAi Consortium) shRNA library (TRCN0000419729) and cloned into the pLKO.1 vector. A scrambled control shRNA vector (pLKO.1-Scrambled) was obtained from Addgene (#136035). The human full-length ADNP in a

lentiviral vector was obtained from Addgene (TFORF-0219). The control vector FUW-M2rtTA was purchased from Addgene (#20342). Lentiviruses were produced in HEK293FT cells (2.5 × 10^6 cells per 10 cm dish) by transfection with 10 µg of the lentiviral transfer vector, 2.5 µg of pMD2.G envelope plasmid, and 7.5 µg of psPAX2 packaging plasmid in Opti-MEM (Gibco, 31985) using Lipofectamine 2000 (Invitrogen, 11668-019). Media containing lentivirus was collected at 24, 36, and 48 h post-transfection. Pooled virus was titrated using a p24 ELISA kit (XpressBIO, XB-1000).

Quantitative real-time PCR

Total RNA was isolated with the Trizol regent (Invitrogen) and converted to cDNA with iScript reverse transcription kit (Bio-Rad). Quantitative RT-PCR was performed on the iCycler iQ Real-Time PCR Detection System (Bio-Rad). The threshold cycle (Ct) value was set when the fluorescence signal reached 10× the s.d. of the baseline. The difference (ΔCt) between the Ct value for target gene and the Ct value for housekeeping gene GAPDH was calculated for each sample, ΔCt = Ct(target)–Ct(GAPDH). The relative level of target gene expression was determined by Fold Change = $2^{-\Delta(\Delta Ct)}$, where Δ(ΔCt) = ΔCt–mean ΔCt (control group). The primers used for quantitative PCR are included in Supplemental Table 2.

Western blotting of nuclear protein

Nuclear extraction was performed as we described before.[23] Briefly, PFC region was dissected and homogenized in 1x hypotonic buffer (20 mM Tris-HCl, pH 7.4, 10 mM NaCl, 3 mM $MgCl_2$, 0.5% NP-40) supplemented with 1 mM PMSF and protease inhibitors. The sample was pipetted up and down six times and passed through a 26-gauge needle four times to disrupt the cell membranes, then incubated on ice for 15 min. The homogenate was centrifuged at 3000 rpm at 4°C for 10 min. The pellet was washed with the hypotonic buffer once, centrifuged again, and resuspend in 50–100 µl 1% SDS solution. After boiling samples, protein concentration was measured.

Samples were loaded for SDS-electrophoresis. Protein signals on the SDS gel were transferred to a nitrocellulose membrane. To detect target proteins, the membrane was incubated overnight with primary antibodies, anti-ADNP (1:1000, ThermoFisher Sci. PA5-52286) and anti-H3 (1:2000, Cell Signal Tech. 4499). After washing, the membrane was incubated with horseradish peroxidase-conjugated secondary antibodies, followed by ECL reaction using enhanced chemiluminescence substrate (Thermo Scientific). Chemidoc XRS system (Bio-Rad) was used to detect luminescence. ImageJ software (NIH) was used to quantify the blot.

Immunostaining

The procedure is similar to what we previously described.[20,24] In brief, after fixation, mouse brains were sectioned into 50 µm coronal slices. Following washing, blocking with 5% Bovine serum albumin (BSA), and permeabilizing with 0.2% Triton X-100, the slices were incubated with primary antibodies overnight at 4°C. The primary antibodies used were anti-ADNP (1:200, PA5-52286, ThermoFisher Sci. USA), and anti-MAP2 (1:5000, ab5392, abcam). Following washing, the slices were incubated with secondary antibodies (1:1000 dilution) for 2 h at room temperature. The secondary antibodies used included AlexaFluor 488 (A-21202), AlexaFluor 568 (A-11041) and AlexaFluor 647 (A-21245) from Invitrogen. The slices were mounted on slides with Vectashield mounting medium. Images were acquired using a Leica TCS SPE confocal microscopy system. under identical conditions. Analysis was performed using Fiji-ImageJ software. An identical threshold was set to remove the background noise, then integrated density (IntDen) was used to measure the intensity of protein fluorescent signal. DAPI was used as an internal reference.

Generation and analysis of human iPSC-derived neurons

Human iPSCs from both normal individuals and early-onset AD patients (4 lines each group) were acquired from the Human Pluripotent Stem Cell Line Repository at the California Institute for Regenerative Medicine (CIRM).

Similar to what we previously described,[24,25] we maintained iPSCs on CF-1 feeders using DMEM/F12 supplemented with 20% KOSR, NEAA (1×), L-glutamine (1×), β-mercaptoethanol (0.1 mM), and FGF2 (4 ng/mL). To initiate differentiation, colonies were dissociated and allowed to form embryoid bodies (EBs). These aggregates were kept in suspension in a 1:1 blend of DMEM/F12 and Neurobasal that included N2 (1:100), NEAA (1×), ascorbic acid (0.2 mM), B27 lacking vitamin A (1:50), and the following morphogens: dorsomorphin dihydrochloride (5 µM), SB431542 (10 µM), cyclopamine (3.5 µM) and XAV939 (2.5 µM). After six days, EBs were transferred onto Matrigel-coated 6-well plates and maintained with media changes every other day until day 12. On day 12, dorsal cortical progenitors were harvested with Accutase (1 U/mL, 37°C) and replated as single cells onto polyornithine/Matrigel-coated dishes at 5000–10,000 cells/cm^2 in a 1:1 DMEM/F12:Neurobasal medium containing N2, ascorbic acid (0.2 mM), NEAA, and B27 without vitamin A. The cultures were again dissociated and replated on day 16 under the same conditions. From day 18 onward, cells were switched to a neuronal maturation medium consisting of Neurobasal with B27 (vitamin A-free, 1:50), GDNF (20 ng/mL), BDNF (20 ng/mL), ascorbic acid (0.2 mM), dcAMP

(0.25 mM), and DAPT (2.5 μM). Half-volume medium changes were performed every other day. Cortical neurons were allowed to mature in this formulation until day 50.

Immunostaining, qPCR and immunoblotting of human iPSC-derived neuronal cultures follow similar procedures with human or mouse tissues. The antibodies used in immunostaining: anti-ADNP (Invitrogen, PA5-52286, 1:1000), anti-CUX1 (Abclonal, A2213, 1:1000), anti-GFAP (Invitrogen, PA5-85109, 1:1000), anti-MAP2 (Abcam, Ab5392, 1:5000), anti-SATB2 (Abclonal, A20220, 1:1000), anti-TBR1 (Proteintech, 20932-I-AP, 1:1000), anti-TAU (Thermo Fisher, AHB0042, 1:1000), and anti-TUJ1 (Abcam, Ab78078, 1:2000).

Statistical analysis

Data were analyzed with GraphPad Prism v.8.4 (GraphPad). Data normality was confirmed using the Shapiro-Wilk test. Comparisons between two independent groups were conducted using two-tailed unpaired Student's t-test. All experiments were replicated in multiple cohorts of animals or iPSC-derived neuronal cultures. All values are mean ± SEM.

Results

Transcriptomic analysis reveals the significant upregulation of complement genes in AD patients

Analysis of the RNA microarray dataset[4] from 230 postmortem human dorsolateral PFC samples (129 late-onset AD; 101 healthy controls) with a cutoff of $p_{adj} \leq 0.05$ and fold change (FC) ≥ 1.2, we identified 278 upregulated genes (Supplemental Table 3). GO enrichment analyses indicated that the most prominently upregulated genes in AD were those involved in immune responses, complement activation and apoptosis (Figure 1A).

Among the most significantly upregulated GO categories in AD—complement, neutrophil immunity, cytokines/inflammation, and apoptosis—protein-protein interaction (PPI) network revealed the rich connections of genes within and between these GO pathways (Figure 1B). Many key genes in the classical complement pathway, including *C1QA, C1QB, C1QC, C4A, C4B, C3, C3AR1,* and *C5AR1*, were significantly elevated in AD, and there were widespread interactions between complement genes (e.g., *C5AR1*) and a number of genes in other GO categories. The Circos plot (Figure 1C), which illustrates DEGs and their connections in each of the 22 chromosomes in a circular layout, also identified complement genes in different chromosomes that are significantly upregulated and closely interconnected. Consistent elevation of many complement gene expression values was observed in the 129 AD patients (Figure 1D), suggesting that complement signaling is altered in AD.

To find out the cell types that have elevated complement gene expression in AD, we analyzed a single-cell transcriptomic dataset from PFC of 48 individuals (15 with early AD pathologies, 9 with late AD pathologies and 24 with no AD pathologies).[5] As shown in Figure 1E, *C1QA, C1QB, C1R, C3AR1, C5AR1*, and other complement components had an increased expression in excitatory neurons, inhibitory neurons, astrocytes or microglia from early AD and pooled AD patients, many of which have reached statistical significance (Supplemental Table 4).

Epigenomic analysis identifies ADNP as the key regulator for complement gene expression

Transcriptomic analysis has identified complement genes as a top-ranking upregulated category in AD, we next used ReMap in ChEA3 Appyter,[26] an integrative analysis of ChIP-seq data for transcriptional regulators from public sources (GEO, ENCODE, ENA), to find out the transcription factors that regulate the expression of complement genes *(C1QA, C1QB, C1QC, C1S, C4A, C4B, C3, C3AR1, C5, C5AR1, CFB, CFH, CFI*). We identified ADNP as one of the top-ranking transcription factors highly associated with the expression of complement genes (Figure 2A, p-value: 0.024, odds ratio: 4.28). ADNP contains nine zinc-fingers at N-terminus and a homeobox domain at C-terminus, suggesting that it has transcription factor activity.[27] ADNP, via recruiting the chromatin architectural protein HP1γ and the chromatin remodeler CHD4, mediates gene repression by modifying chromatin accessibility.[17]

Comparing gene targets that have ADNP binding at their promoters (±5Kb TSS) identified from ChIP-seq (4453, ChIP-Atlas) with upregulated genes in AD postmortem PFC identified from the microarray dataset (1177, $p_{adj} \leq 0.05$, FC ≥ 1.1), we found that 229 ADNP targets were elevated in AD, including complement genes *C1QB, C3, C3AR1, C4B,* and *C5AR1* (Figure 2B, Supplemental Table 5), These genes were most enriched in apoptotic regulation, cytokine response, NFκB signaling and phagocytosis (Figure 2C).

To find out whether complement gene transcription is directly linked to ADNP, we used Integrative Genomics Viewer (IGV) to examine ADNP occupancy at the loci of complement genes. The snapshots of human ADNP ChIP-seq (GEO accession: GSM2827324) landscapes revealed ADNP peaks at the promoter (marked by H3K4me3) or enhancer (marked by H3K27ac) regions of *C1QA*, *C1QB, and C3AR1* (Figure 2D). It suggests that ADNP could directly bind to complement genes, repressing their transcription.

ADNP expression is significantly diminished in AD

Given the potential link of ADNP/HP1γ to complement gene regulation revealed by epigenomic analyses, we next

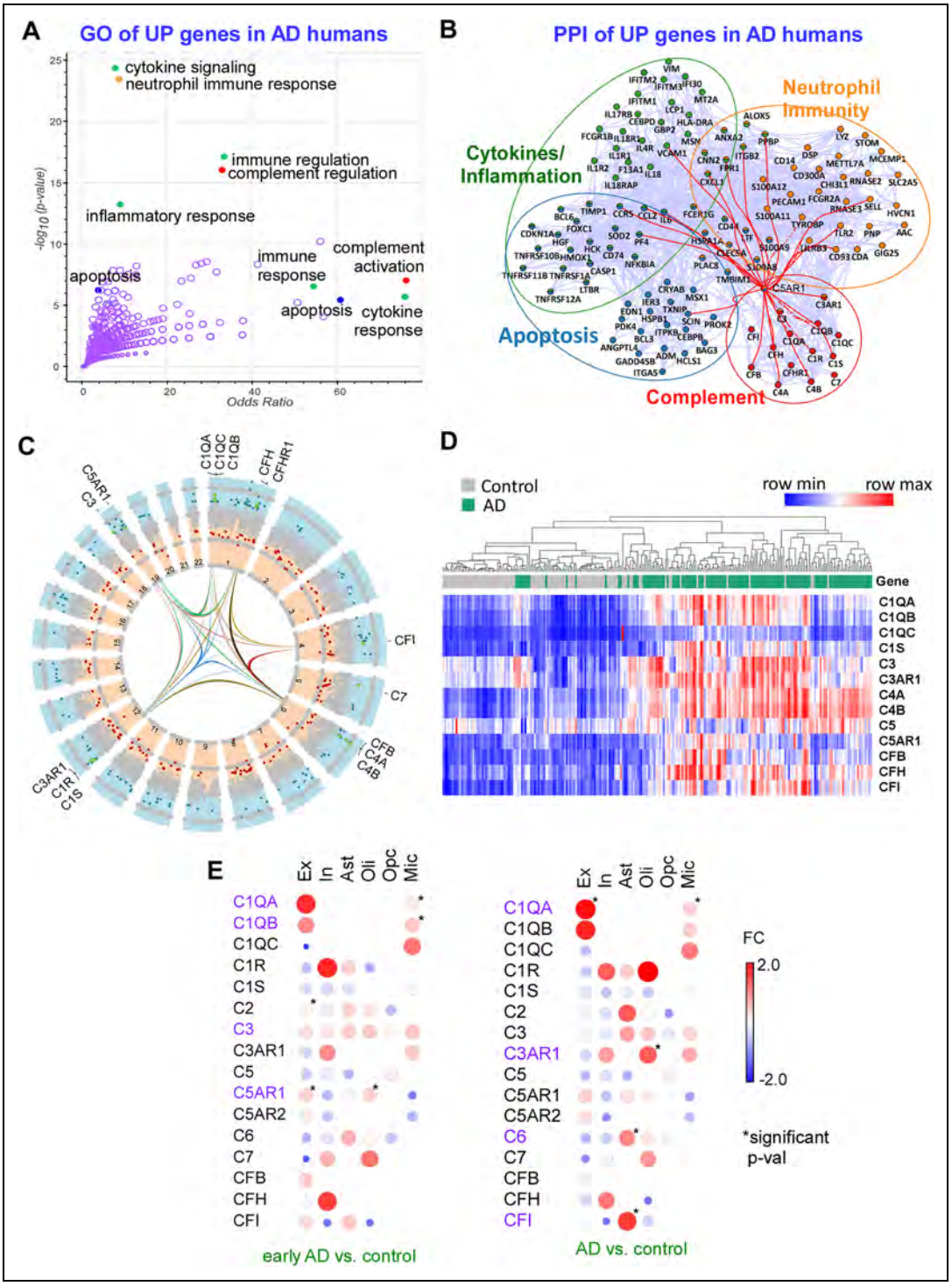

Figure 1. Complement genes are significantly upregulated in PFC of AD patients from transcriptomic analysis. (A) Enrichment analysis of upregulated DEGs in postmortem PFC from 129 AD patient samples, compared to 101 control humans. The enriched gene ontology (GO) pathways with the most significant changes (p value and odds ratio) are highlighted. (B) Interaction network of the upregulated genes among the four major GO pathways in AD patients. (C) Circos plots showing genes in each of the 19 chromosomes with upregulated (blue dots) and downregulated (red dots) transcription in AD patients. Upregulated complement genes in each chromosome are labeled on the outside. (D) Heatmaps generated from Phantasus showing complement gene expression values in postmortem PFC from control versus AD patients. (E) Heatmaps showing the changes of complement genes in PFC of early AD or pooled AD patients, compared to control humans. The color and size of circles reflect the fold change (FC). Significant changes ($p \leq 0.05$) are labeled with *. Ex: excitatory neurons; In: inhibitory neurons; Ast: astrocytes; Oli: oligodendrocytes; Opc: oligodendrocyte progenitor cells; Mic: microglia. (Color figure available online).

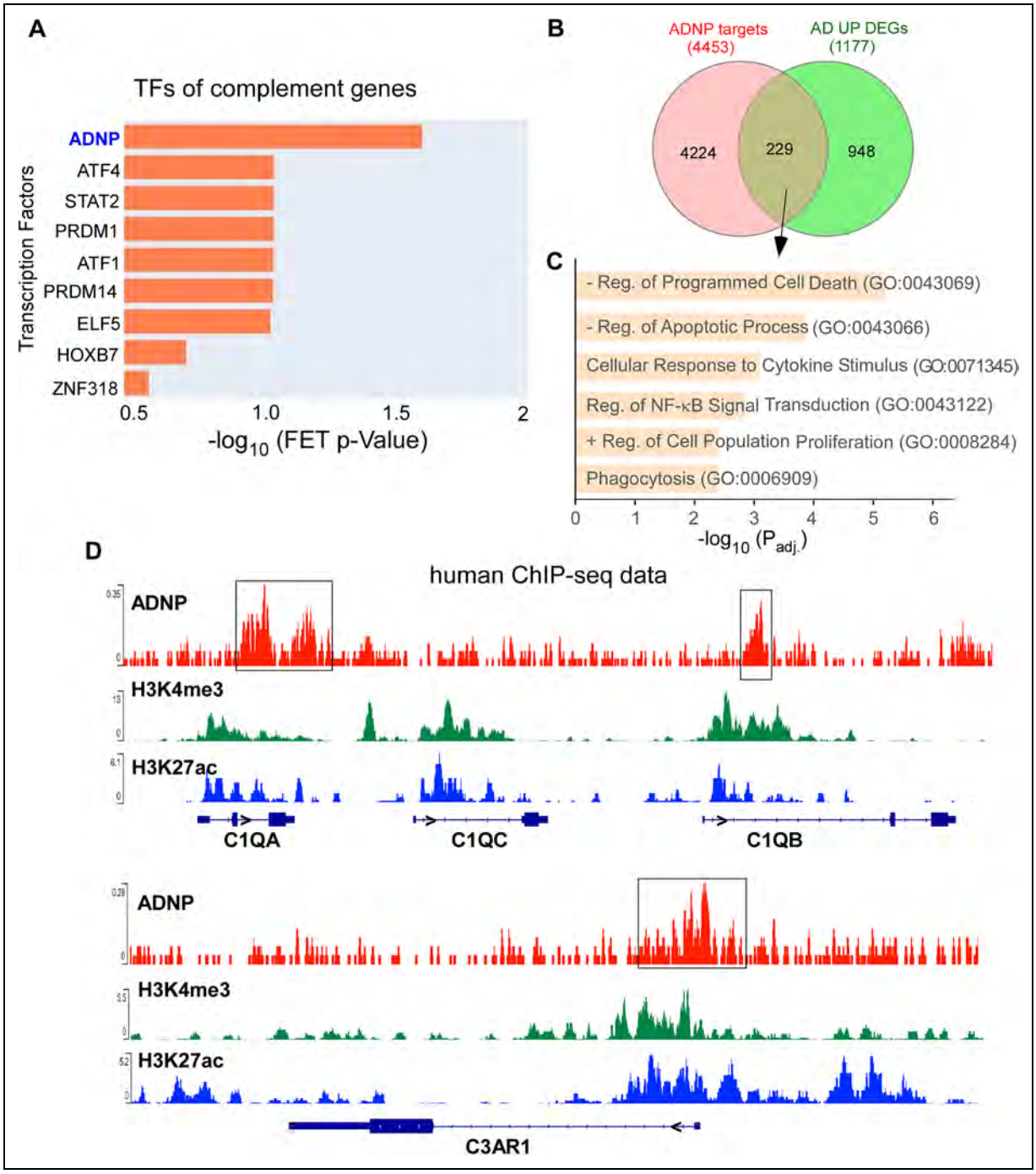

Figure 2. ADNP is a top-ranking transcription factor for elevated complement genes in ad, and ADNP is enriched at complement genes. (A) Top predicted upstream transcription factors regulating the elevated complement genes in AD. (B) Venn diagrams showing the overlap of gene targets of ADNP with upregulated genes in AD. (C) Bar graphs showing GO pathways of AD-related gene targets of ADNP. (D) Epigenome browser of ADNP ChIP-seq enrichment at *C1qa, C1qb* and *C3ar1* promoter or enhancer regions (highlighted with boxes). (Color figure available online).

examined the possible alteration of ADNP and HP1γ in AD. Postmortem PFC tissues (*BA10*) from AD patients versus age and sex-matched control subjects (NIH Neurobiobank) were used. Demographic data of these postmortem human samples are included in our previous publications.[28,29] We found that the mRNA level of *ADNP* and *HP1γ* was substantially reduced in human AD samples (Figure 3A, n = 12 per group, *ADNP*: 44% reduction, p = 0.01, *HP1γ*, 31.4% reduction, p = 0.025, t-test). In PFC of 8-month-old 5xFAD mice, a familial AD

model with 5 mutations on APP/PS1, *Adnp* mRNA was also reduced, while *Hp1γ* was not altered (Figure 3B, n = 12–13 per group for *Adnp*, 22% reduction, $p < 0.05$, t-test).

We further performed Western blotting to compare ADNP protein levels in the nuclear fraction of PFC from control versus AD postmortem tissues. As shown in Figure 3C, the full-length ADNP was significantly decreased in AD human samples (n = 6 per group, 55% reduction, $p = 0.04$, t-test). In addition, we performed immunocytochemistry experiments to compare ADNP in PFC of WT versus 5xFAD mice. As shown in Figure 3D, the fluorescent signal of ADNP was significantly lower in PFC slices from 5xFAD mice than those from WT mice (n = 24 images from 6 slices of 3 mice per group, 33.6% decrease, $p = 0.0002$, t-test). These data suggest that ADNP expression is downregulated in AD.

Complement genes are convergent targets of ADNP deficiency and AD

With the reduction of ADNP in AD patients, we next generated mice with ADNP knockdown (KD) in the PFC, and examined transcriptomic consequences. AAV carrying the GFP-tagged *ADNP* shRNA was injected into the medial PFC bilaterally of wild-type mice. Our previous study has confirmed the in vivo knockdown of ADNP.[20]

To find out what gene alterations are commonly present in ADNP-deficient and AD conditions, we used Appyter Set Comparison to compare the upregulated genes in PFC from mice with ADNP knockdown (967, $p \leq 0.05$, $FC \geq 1.2$),[20] 5xFAD mice (877, $p \leq 0.05$, $FC \geq 1.2$) and human AD brains (278, $p_{adj} \leq 0.05$, $FC \geq 1.2$).[4] We identified 37 common genes with significantly elevated expression in all three groups (Figure 4A, Supplemental Table 6). Enrichment analysis (Appyter) revealed that the most enriched convergent pathway among the 37 common genes was the regulation of complement activation (Figure 4B). PPI network of the 37 common genes (Figure 4C) indicated their inter-connections among four major categories—complement, immunity, cytokine, and apoptosis.

Next, we performed Hub analysis to identify top ranking genes that are common to the three groups of DEGs (ADNP knockdown, 5xFAD and AD patients) and have the highest intra-molecular connectivity. Interestingly, several complement genes, such as C1QA, C1QB, C1QC, C3AR1, and C5AR1, were among the central hub genes identified (Figure 4D).

Next, we performed qPCR experiments to profile complement genes in PFC from postmortem AD humans, 5xFAD mice and ADNP knockdown mice. As shown in Figure 4E, the mRNA level of *C3, C1QA, C3AR1* and *C5AR1* was significantly elevated in AD humans (n = 8–11 per group, *C1QA:* $p = 0.03$, *C3*: $p = 0.0001$, *C3AR1*, $p = 0.002$, *C5AR1*: $p = 0.01$, t-test). Significantly elevated mRNA level of complement genes was also found in 5xFAD (8-month-old) mice (Figure 4F, n = 6–9 per group, *C1qa:* $p = 0.0001$, *C3ar1,* $p = 0.0003$, *C5ar1*: $p = 0.0004$, t-test) and ADNP knockdown (6-month-old) mice (Figure 4G, n = 6 per group, *Adnp*: $p = 0.018$, *C1qa:* $p = 0.0001$, *C3*: $p = 0.04$, *C3ar1*, $p = 0.0001$, *C5ar1*: $p = 0.001$, t-test). These data indicate that the upregulation of complement genes in PFC is a converging transcriptomic aberration in ADNP-deficient and AD conditions.

AD patient-derived neuronal cultures exhibit astrocyte activation and altered ADNP/complement gene expression

To find out translational values of the results from AD mouse models, human iPSC lines have often been used.[30,31] Thus, we generated iPSC-derived cortical neuronal cultures from four early-onset AD patients and four control subjects, and examined whether they exhibited similar epigenetic and cellular alterations as in the FAD mouse model and AD postmortem tissues.

Using a method that we developed,[25] human iPSCs were differentiated to embryoid bodies (EBs) in suspension culture in the presence of the dual SMAD inhibitors SB431542 and dorsomorphin to drive cells to the neural lineage.[32] The WNT signaling inhibitor XAV939 was used to rostralize the cell fate,[33,34] while the SHH antagonist cyclopamine was used to dorsalize the cells.[35] The resulting cortical neural progenitor cells (NPCs) produced neural rosettes resembling the cross-section of the neural tube. Cortical NPCs were then differentiated to cortical neurons expressing MAP2, as well as neuronal markers TUJ1 and TAU and various cortical layer markers TBR1, CUX1 and SATB2 (Figure 5A).

Reactive astrocytes, which are activated astrocytes involved in brain inflammation, are a major source of complement components like C3 and C1q.[36] We next examined whether AD iPSC-derived cortical neuronal cultures had activated astrocytes. Our immunostaining of AD human iPSC-derived cortical neuronal cultures revealed the significantly increased astrocyte marker GFAP signal intensity and GFAP-positive cell counts (Figure 5B and 5C, n = 20 images of cultures from 4 lines per group, all $p < 0.001$, t-test). These data suggest that a prominent AD pathology, astrogliosis, is recapitulated by these iPSC-derived neuronal cultures.

Our qPCR and western blotting studies found that iPSC-derived neuronal cultures from AD patients exhibited the significantly reduced *ADNP* and *HP1γ* mRNA levels (Figure 6A, n = 10 cultures from 4 lines per group, ADNP: 43.2% reduction, $p = 0.0034$; *HP1γ*: 45.3% reduction, $p = 0.0002$, t-test), as well as the significantly reduced ADNP protein levels (Figure 6B, n = 3 lines per group, 60% reduction, $p = 0.015$, t-test), compared to

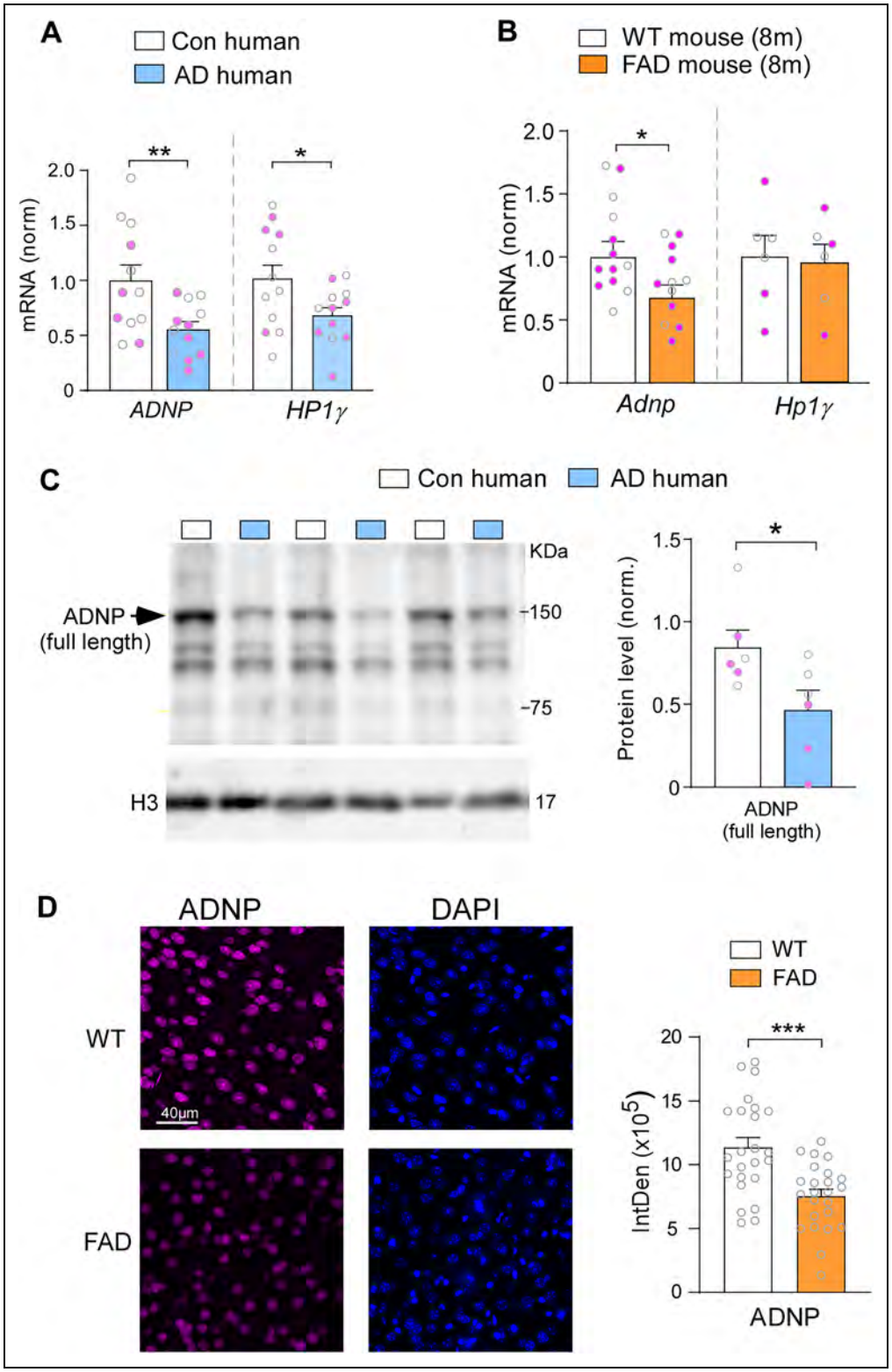

Figure 3. ADNP expression is reduced in PFC of postmortem AD humans and 5xFAD mice. (A, B) Bar graphs showing qPCR data of the mRNA level of ADNP and HP1γ in PFC of postmortem tissue from control versus AD humans (A) or WT versus 5xFAD mice (B). Females are labeled with pink dots. (C) Representative western blots and bar graphs showing the protein level of ADNP in PFC of postmortem tissue from control (C) versus AD (A) humans. Females are labeled with pink dots. (D) Representative confocal images of PFC slices stained with ADNP and DAPI. Inset: Bar graphs showing the integrated density of ADNP fluorescent signals in PFC slices of WT versus 5xFAD mice. ***$p < 0.001$, t-test. (Color figure available online).

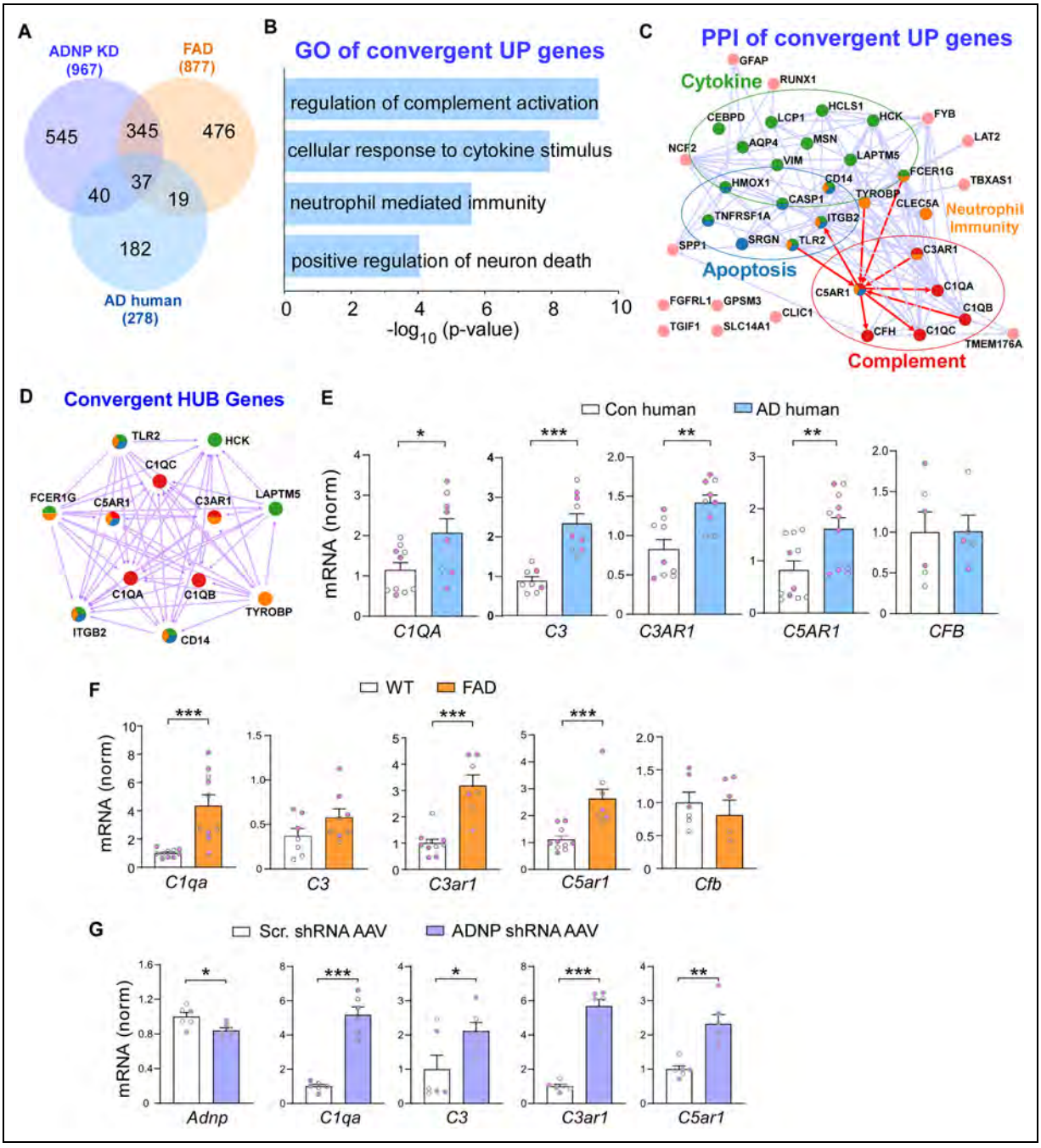

Figure 4. Complement genes are commonly upregulated in PFC from ADNP-deficient mice, 5xFAD mice and AD patients. (A) Venn diagram showing the overlapping of upregulated genes by ADNP knockdown (KD) with the elevated genes in 5xFAD mice and AD patients. (B, C) Enriched pathways (B) and interaction network (C) of the 37 commonly upregulated (UP) genes. (D) Hub genes identified from the 37 common UP genes and their interaction networks. (E-G) Bar graphs showing qPCR data of the mRNA level of complement genes in PFC of postmortem tissue from control subjects versus AD patients (E), WT versus 5xFAD mice (F), and mice injected with control versus ADNP shRNA AAV (G). Females are labeled with pink dots. *$p < 0.05$, **$p < 0.01$, ***$p < 0.001$, t-test. (Color figure available online).

those from control subjects. Immunostaining of AD human iPSC-derived cortical neuronal cultures revealed the significantly decreased ADNP signal intensity and ADNP-positive cell counts (Figure 6C and 6D, $n = 20$ images of cultures from 4 lines per group, intensity: $p = 0.0015$, count: $p = 0.034$, t-test). Furthermore, the mRNA level of complement genes *C1QA, C3AR1,* and *C5AR1* was significantly increased in AD iPSC-derived neuronal

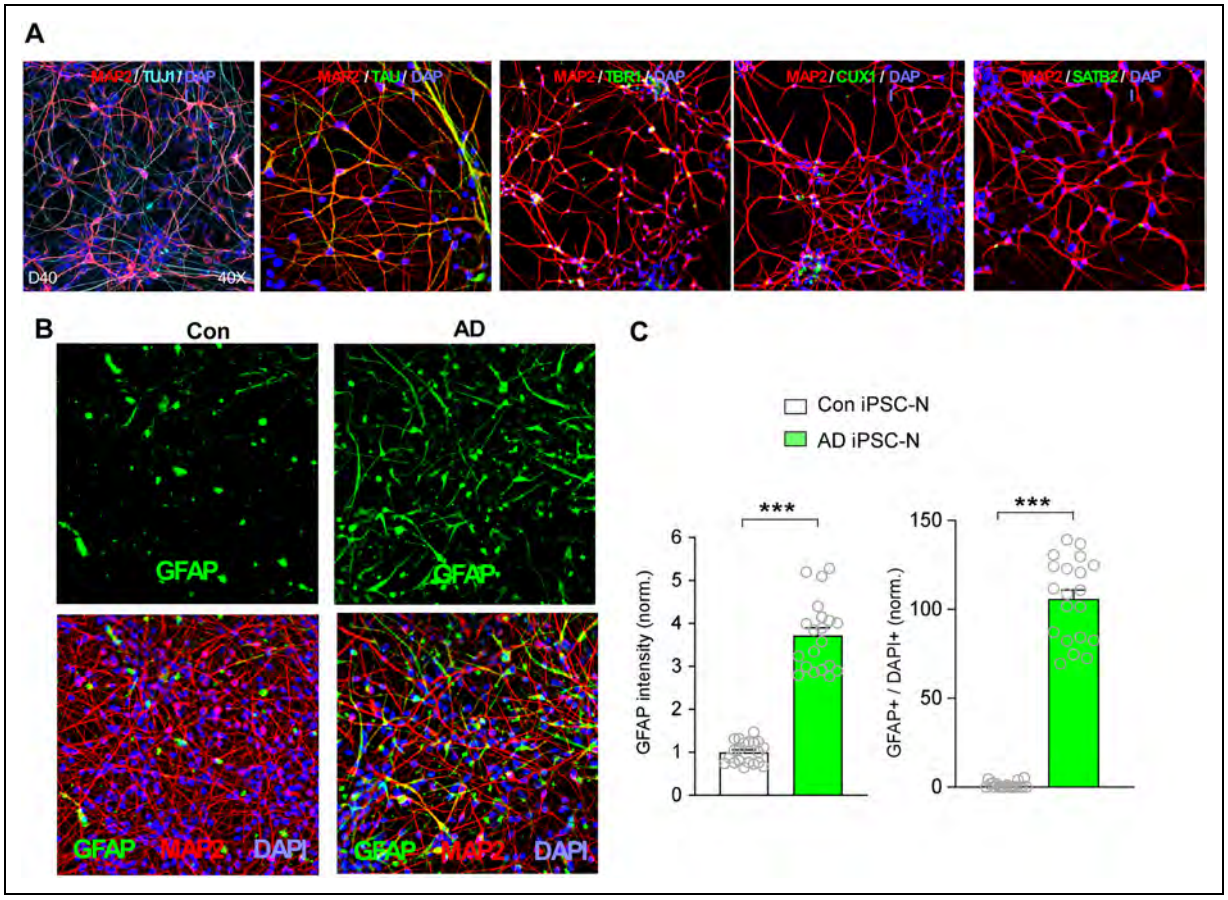

Figure 5. Ad patient-derived cortical neuronal cultures have astrocyte activation. (A) Images of iPSC-derived neuronal cultures stained with neuronal markers (MAP2, TUJ1 and TAU) and various cortical layer markers (TBR1, CUX1 and SATB2). (B) Images of iPSC-derived neuronal cultures stained with GFAP from a control and an AD patient. (C) Quantification of GFAP intensity and GFAP + cell counts in iPSC-derived neuronal cultures from controls versus AD patients. DAPI was used for quantification and normalization. ***$p < 0.001$, t-test. (Color figure available online).

cultures (Figure 6E, n = 7 cultures from 4 lines per group, *C1QA*: 73.1% increase, p = 0.0015; *C3AR1*: 63.0% increase, p = 0.0012; *C5AR1*: 65.2% increase, p = 0.0001, t-test), recapturing what was found in ADNP-deficient mice, postmortem AD humans and 5xFAD mice.

Finally, we manipuated ADNP levels in iPSC-derived neuronal cultures from control or AD patients to evaluate the direct impact of ADNP on complement genes. When control cells were infected with ADNP shRNA lentivirus to knockdown ADNP, complement genes were significantly increased (Figure 6F; $n = 4$ cultures from 2 control lines per group, *ADNP*: 46.2% decrease, $p = 0.0004$; *C1QA*: 208% increase, $p = 0.003$; *C3AR1*: 244% increase, $p = 0.006$; *C5AR1*: 188% increase, $p = 0.008$; *t*-test). Conversely, when AD cells were infected with full-length ADNP lentivirus to elevate ADNP, complement genes were significantly decreased (Figure 6G; $n = 4$ cultures from 2 AD lines per group; *ADNP*: 55% increase, $p = 0.002$; *C1QA*: 46% decrease, $p = 0.009$; *C3AR1*: 48% decrease, $p = 0.001$; *C5AR1*: 42% decrease, $p = 0.007$; *t*-test). These bi-directional results have further demonstrated the role of ADNP in regulating complement gene expression.

Discussion

In AD, complement genes are among the top-ranking transcriptionally upregulated genes.[3] Complement components could be secreted by reactive astrocytes[12,36] or expressed in stressed neurons and bind to synaptic proteins.[7,11,37] Binding of C1q to its target induces the formation of an activated enzyme complex that can lead to the cleavage of C2 and the subsequent cleavage of C3 into C3a and C3b, which can bind to their receptors C3aR and CR3, respectively. C3b then binds to the existing C3 convertase to form a C5 convertase, which cleaves C5 into C5a and C5b. Complement-tagged neurons can be recognized by complement receptors on microglia, leading to synapse elimination

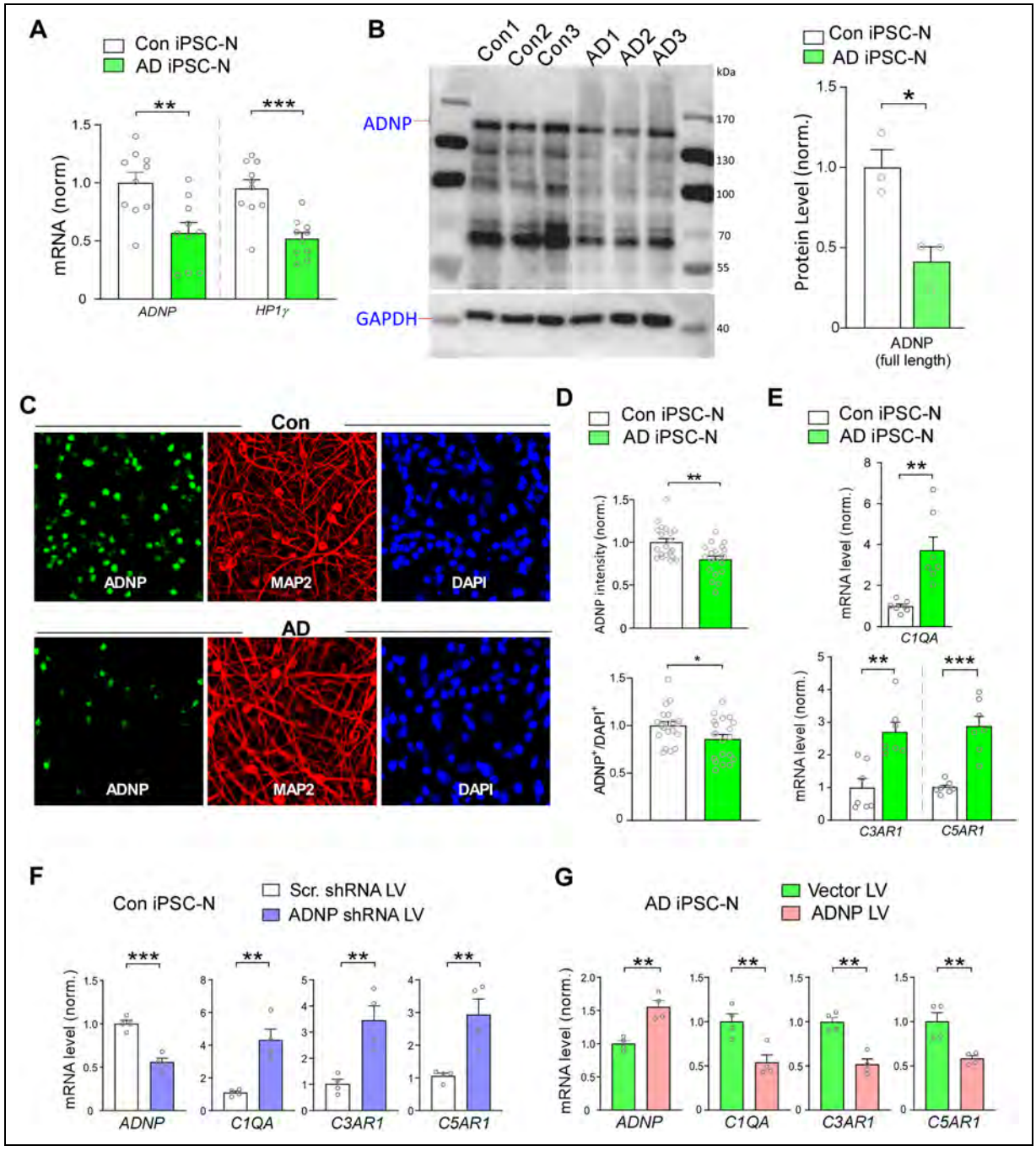

Figure 6. Ad patient-derived cortical neuronal cultures have decreased ADNP expression and increased complement gene transcription. (A) Quantitative PCR data showing the mRNA level of ADNP and HP1γ in iPSC-derived neuronal cultures from controls versus AD patients. (B) Western blots and bar graphs showing the protein level of ADNP in iPSC-derived neuronal cultures from controls versus AD patients. (C) Images of iPSC-derived neuronal cultures stained with ADNP, MAP2 and DAPI from a control and an AD patient. (D) Quantification of ADNP intensity and ADNP + cell counts in iPSC-derived neuronal cultures from controls versus AD patients. DAPI was used for quantification and normalization. (E) Quantitative PCR data showing the mRNA level of complement genes (C1QA, C3AR1, and C5AR1) in iPSC-derived neuronal cultures from controls versus AD patients. (F, G) Quantitative PCR analysis showing mRNA levels of ADNP and complement genes (C1QA, C3AR1, and C5AR1) in iPSC-derived cortical neuronal cultures from either two control lines infected with scrambled shRNA versus ADNP shRNA lentivirus (F) or from two AD lines infected with empty vector versus full-length ADNP lentivirus (G). *$p < 0.05$, **$p < 0.01$, ***$p < 0.001$, t-test. (Color figure available online).

by phagocytosis.[7,11] Thus, microglia activation increases susceptibility to neurodegeneration.[38,39] Here we demonstrate the significantly increased complement genes in AD postmortem cortex and 5xFAD mouse model. Moreover, AD patient-derived neuronal cultures recapitulate astrocyte activation and exhibit the elevation of complement genes, supporting the notion that the dysregulation of neuron-glia interaction through complement signaling is potentially linked to synaptic dysfunction and neurodegeneration in AD.[7,11,36,37]

Our epigenomic analysis identifies ADNP as a top-ranking transcription factor regulating complement gene expression, and ADNP is enriched at the promoter regions of complement genes. We have found that ADNP mRNA level and nuclear protein level are significantly diminished in AD postmortem cortex, 5xFAD mice and AD patient-derived neuronal cultures (iPSC-N). Knockdown of ADNP in wild-type mice leads to a significant increase of complement gene expression. In addition, knockdown of ADNP in iPSC-N from control subjects leads to complement gene upregulation, while overexpression of ADNP in iPSC-N from AD patients leads to complement gene reduction. These data suggest that ADNP deficiency in AD contributes to the elevation of complement genes.

The reduction of dendritic spine density has been found in ADNP$^{+/-}$ mice,[40] while neuronal numbers are not significantly changed by ADNP knockdown in mouse PFC.[20] Thus, ADNP deficiency-induced complement gene elevation may cause synapse pruning, not neuronal loss, via microglial/astrocyte activation.

How might ADNP regulate complement gene transcription? ADNP has physical association with chromatin remodelers, which play a key role in dynamically modifying chromatin structure via controlling nucleosome assembly, editing and organization.[41,42] ADNP forms a complex with HP1γ and CHD4 to mediate gene silencing by establishing inaccessible chromatin around its DNA-binding sites.[17] ADNP also regulates local chromatin architecture by competing for binding with the genome architecture protein CTCF.[43] ADNP may suppress the expression of complement genes via reducing chromatin accessibility or blocking chromatin loop formation at their promoter and enhancer regions. The detailed mechanisms await to be further studied.

ADNP is a top-ranking risk gene for ID and autism.[13–16] Our previous studies have found that Adnp deficiency in mouse PFC induces impaired cognitive task performance, upregulation of genes enriched in neuroinflammation, increased pro-phagocytic microglial activation, and decreased glutamatergic transmission and postsynaptic protein expression.[20] ADNP also has several unique aging/AD mutations and the frequency of an ADNP mutation in AD is found to be correlated with tauopathy.[44] The role of ADNP in AD is largely focused on its impact on axonal transport via interacting with microtubule-binding proteins.[45] Our current study has revealed a novel mechanism related to ADNP function in the nucleus, which is to restrain the transcription of complement genes, protecting neurons against synapse loss by microglia/astrocyte activation. The attenuation of such a function of ADNP may contribute to AD pathophysiology.

Acknowledgements

We thank Xiaoqing Chen, Dr Ping Zhong and Rachel Senek for their technical support.

ORCID iDs

Zhen Yan https://orcid.org/0000-0002-3519-9596
Yong Ren https://orcid.org/0000-0001-9771-1084

Ethical considerations

Not applicable.

Consent to participate

Not applicable.

Consent for publication

Not applicable.

Author contribution(s)

Yong Ren: Data curation; Formal analysis; Investigation; Writing – review & editing.
Komal Saleem: Data curation; Formal analysis; Investigation; Writing – review & editing.
Prachetas Jai Patel: Data curation; Formal analysis; Methodology.
Young-Ho Lee: Data curation; Formal analysis.
Jian Feng: Methodology; Supervision.
Zhen Yan: Conceptualization; Funding acquisition; Project administration; Writing – original draft; Writing – review & editing.

Funding

The authors disclosed receipt of the following financial support for the research, authorship, and/or publication of this article: This work was supported by a grant from Department of Veteran Affairs (grant number: I01-BX006357) to Z.Y.

Declaration of conflicting interests

The authors declared no potential conflicts of interest with respect to the research, authorship, and/or publication of this article.

Data availability statement

Data will be made available on request.

Supplemental material

Supplemental material for this article is available online.

References

1. Gan L, Cookson MR, Petrucelli L, et al. Converging pathways in neurodegeneration, from genetics to mechanisms. *Nat Neurosci* 2018; 21: 1300–1309.
2. Nichols MR, St-Pierre MK, Wendeln AC, et al. Inflammatory mechanisms in neurodegeneration. *J Neurochem* 2019; 149: 562–581.
3. Bai B, Wang X, Li Y, et al. Deep multilayer brain proteomics identifies molecular networks in Alzheimer's disease progression. *Neuron* 2020; 105: 975–991.e977.
4. Zhang B, Gaiteri C, Bodea LG, et al. Integrated systems approach identifies genetic nodes and networks in late-onset Alzheimer's disease. *Cell* 2013; 153: 707–720.
5. Mathys H, Davila-Velderrain J, Peng Z, et al. Single-cell transcriptomic analysis of Alzheimer's disease. *Nature* 2019; 570: 332–337.
6. Zhou Y, Song WM, Andhey PS, et al. Human and mouse single-nucleus transcriptomics reveal TREM2-dependent and TREM2-independent cellular responses in Alzheimer's disease. *Nat Med* 2020; 26: 131–142.
7. Dalakas MC, Alexopoulos H and Spaeth PJ. Complement in neurological disorders and emerging complement-targeted therapeutics. *Nat Rev Neurol* 2020; 16: 601–617.
8. Stephan AH, Barres BA and Stevens B. The complement system: an unexpected role in synaptic pruning during development and disease. *Annu Rev Neurosci* 2012; 35: 369–389.
9. Tenner AJ. Complement-mediated events in Alzheimer's disease: mechanisms and potential therapeutic targets. *J Immunol* 2020; 204: 306–315.
10. Tenner AJ, Stevens B and Woodruff TM. New tricks for an ancient system: physiological and pathological roles of complement in the CNS. *Mol Immunol* 2018; 102: 3–13.
11. Hong S, Beja-Glasser VF, Nfonoyim BM, et al. Complement and microglia mediate early synapse loss in Alzheimer mouse models. *Science* 2016; 352: 712–716.
12. Wu T, Dejanovic B, Gandham VD, et al. Complement C3 is activated in human AD brain and is required for neurodegeneration in mouse models of amyloidosis and tauopathy. *Cell Rep* 2019; 28: 2111–2123.e2116.
13. Stessman HA, Xiong B, Coe BP, et al. Targeted sequencing identifies 91 neurodevelopmental-disorder risk genes with autism and developmental-disability biases. *Nat Genet* 2017; 49: 515–526.
14. Satterstrom FK, Kosmicki JA, Wang J, et al. Large-scale exome sequencing study implicates both developmental and functional changes in the neurobiology of autism. *Cell* 2020; 180: 568–584.e523.
15. Fitzgerald TW, Gerety SS, Jones WD, et al. Large-scale discovery of novel genetic causes of developmental disorders. *Nature* 2015; 519: 223–228.
16. McRae JF, Clayton S, Fitzgerald TW, et al. Prevalence and architecture of de novo mutations in developmental disorders. *Nature* 2017; 542: 433–438.
17. Ostapcuk V, Mohn F, Carl SH, et al. Activity-dependent neuroprotective protein recruits HP1 and CHD4 to control lineage-specifying genes. *Nature* 2018; 557: 739–743.
18. Hadar A, Kapitansky O, Ganaiem M, et al. Introducing ADNP and SIRT1 as new partners regulating microtubules and histone methylation. *Mol Psychiatry* 2021; 26: 6550–6561.
19. Oakley H, Cole SL, Logan S, et al. Intraneuronal beta-amyloid aggregates, neurodegeneration, and neuron loss in transgenic mice with five familial Alzheimer's disease mutations: potential factors in amyloid plaque formation. *J Neurosci* 2006; 26: 10129–10140.
20. Conrow-Graham M, Williams JB, Martin J, et al. A convergent mechanism of high risk factors ADNP and POGZ in neurodevelopmental disorders. *Brain* 2022; 145: 3250–3263.
21. Xie Z, Bailey A, Kuleshov MV, et al. Gene set knowledge discovery with enrichr. *Curr Protoc* 2021; 1: e90.
22. Robinson JT, Thorvaldsdóttir H, Winckler W, et al. Integrative genomics viewer. *Nat Biotechnol* 2011; 29: 24–26.
23. Qin L, Ma K, Wang ZJ, et al. Social deficits in Shank3-deficient mouse models of autism are rescued by histone deacetylase (HDAC) inhibition. *Nat Neurosci* 2018; 21: 564–575.
24. Yang G, Ren Y, Zhong P, et al. Histone demethylase PHF2 regulates inflammatory genes in Alzheimer's disease. *Mol Psychiatry* 2025; 31: 845–859.
25. Jiang H, Xiao Z, Saleem K, et al. Generation of human induced pluripotent stem cell-derived cortical neurons expressing the six tau isoforms. *J Alzheimers Dis* 2025; 105: 1341–1354.
26. Keenan AB, Torre D, Lachmann A, et al. ChEA3: transcription factor enrichment analysis by orthogonal omics integration. *Nucleic Acids Res* 2019; 47: W212–W224.
27. Zamostiano R, Pinhasov A, Gelber E, et al. Cloning and characterization of the human activity-dependent neuroprotective protein. *J Biol Chem* 2001; 276: 708–714.
28. Cao Q, Wang W, Williams JB, et al. Targeting histone K4 trimethylation for treatment of cognitive and synaptic deficits in mouse models of Alzheimer's disease. *Sci Adv* 2020; 6: eabc8096.
29. Williams JB, Cao Q, Wang W, et al. Inhibition of histone methyltransferase Smyd3 rescues NMDAR and cognitive deficits in a tauopathy mouse model. *Nat Commun* 2023; 14: 91.
30. McQuade A, Kang YJ, Hasselmann J, et al. Gene expression and functional deficits underlie TREM2-knockout microglia responses in human models of Alzheimer's disease. *Nat Commun* 2020; 11: 5370.
31. Bassil R, Shields K, Granger K, et al. Improved modeling of human AD with an automated culturing platform for iPSC neurons, astrocytes and microglia. *Nat Commun* 2021; 12: 5220.
32. Chambers SM, Fasano CA, Papapetrou EP, et al. Highly efficient neural conversion of human ES and iPS cells by dual inhibition of SMAD signaling. *Nat Biotechnol* 2009; 27: 275–280.

33. Nicoleau C, Varela C, Bonnefond C, et al. Embryonic stem cells neural differentiation qualifies the role of Wnt/β-Catenin signals in human telencephalic specification and regionalization. *Stem Cells* 2013; 31: 1763–1774.
34. Puelles L and Rubenstein JL. Expression patterns of homeobox and other putative regulatory genes in the embryonic mouse forebrain suggest a neuromeric organization. *Trends Neurosci* 1993; 16: 472–479.
35. Lai K, Kaspar BK, Gage FH, et al. Sonic hedgehog regulates adult neural progenitor proliferation in vitro and in vivo. *Nat Neurosci* 2003; 6: 21–27.
36. Lian H, Yang L, Cole A, et al. NFκB-activated astroglial release of complement C3 compromises neuronal morphology and function associated with Alzheimer's disease. *Neuron* 2015; 85: 101–115.
37. Luchena C, Zuazo-Ibarra J, Alberdi E, et al. Contribution of neurons and glial cells to complement-mediated synapse removal during development, aging and in Alzheimer's disease. *Mediators Inflamm* 2018; 2018: 2530414.
38. Thion MS, Ginhoux F and Garel S. Microglia and early brain development: an intimate journey. *Science* 2018; 362: 185–189.
39. Salter MW and Stevens B. Microglia emerge as central players in brain disease. *Nat Med* 2017; 23: 1018–1027.
40. Hacohen-Kleiman G, Sragovich S, Karmon G, et al. Activity-dependent neuroprotective protein deficiency models synaptic and developmental phenotypes of autism-like syndrome. *J Clin Invest* 2018; 128: 4956–4969.
41. Chen T and Dent SY. Chromatin modifiers and remodellers: regulators of cellular differentiation. *Nat Rev Genet* 2014; 15: 93–106.
42. Clapier CR, Iwasa J, Cairns BR, et al. Mechanisms of action and regulation of ATP-dependent chromatin-remodelling complexes. *Nat Rev Mol Cell Biol* 2017; 18: 407–422.
43. Kaaij LJT, Mohn F, van der Weide RH, et al. The ChAHP complex counteracts chromatin looping at CTCF sites that emerged from SINE expansions in mouse. *Cell* 2019; 178: 1437–1451.e1414.
44. Ivashko-Pachima Y, Hadar A, Grigg I, et al. Discovery of autism/intellectual disability somatic mutations in Alzheimer's brains: mutated ADNP cytoskeletal impairments and repair as a case study. *Mol Psychiatry* 2021; 26: 1619–1633.
45. Ivashko-Pachima Y and Gozes I. Activity-dependent neuroprotective protein (ADNP)-end-binding protein (EB) interactions regulate microtubule dynamics toward protection against tauopathy. *Prog Mol Biol Transl Sci* 2021; 177: 65–90.